Bias-induced change in effective mobility observed in polymer transistors

R. A. Street*
Palo Alto Research Center, 3333 Coyote Hill Road, Palo Alto, California 94304, USA
(Received 15 January 2008; revised manuscript received 3 March 2008; published 7 April 2008)

Changes in the mobility induced by an extended application of a gate bias are reported in polythiophene thin film transistors. The gate-induced decrease in mobility is unrelated to the previously studied threshold shift effect that arises from trapped holes. The mobility decrease has a strong temperature dependence, is irreversible by low temperature annealing, and depends on the number of times the gate is switched as well as the duration of the gate bias. The effect exhibits both as an increase in series resistance and as a change in bulk mobility. The thermal activation of the process suggests an energy barrier to a new physical structure which is too stable to reverse. A possible mechanism for structural changes is proposed, based on the electrostrictive effect.

DOI: 10.1103/PhysRevB.77.165311 PACS number(s): 72.80.Le, 85.30.Tv

I. INTRODUCTION

The changes that occur during operation of a polymer thin film transistor (TFT) are important for technology applications and interesting for an improved understanding of the material properties. Several recent papers describe the bias-stress effects on the threshold voltage.[1–5] In particular, we previously showed that the application of a low duty cycle pulsed gate accumulation bias stress to a polythiophene TFT causes a threshold voltage (V_T) shift which increases over about 1–2 days at room temperature and then stabilizes at an approximately constant value.[6] The V_T shift recovers after the stress is removed with a time constant of a few days at room temperature. During extended measurements, it was noticed that the gate stress also induces a slow decrease in the slope of the transfer characteristics, which continues over at least several months, indicating an apparent stress-induced change in mobility. A similar effect was observed for samples held in either clean dry air or dry nitrogen. This paper characterizes the stress-induced change in effective mobility in more detail and extends the measurements to another polythiophene semiconductor.

Various changes in the mobility of organic TFTs have been reported, for reasons other than bias stress.[7,8] The mobility is highly sensitive to structural changes in the semiconductor, and most of the improvement in TFT performance over the past several years has been a result of improved control of the structure.[9] Chemical exposure to various volatile compounds decreases the mobility, an effect that may also be due to disordering of the structure.

II. MEASUREMENTS

Measurements were made on polythiophene bottom gate, bottom contact TFTs. The semiconductors studied are poly(3,3‴-didodecylquarterthiophene) (PQT-12)[10] and poly(2,5-bis(3-alkylthiophen-2yl)thieno[3,2-b]thiophene) (PBTTT).[9] The devices have a 300 nm plasma-enhanced chemical-vapor deposition silicon oxide/nitride dielectric (capacitance of ~20 nF/cm^2) and chrome/gold coplanar bottom contacts. The gate, source, and drain contacts are first made by photolithography, then the polymer semiconductor is spin coated or drop cast, and the devices are unencapsulated. Channel lengths range from 5 to 50 μm, and widths from 150 to 500 μm, with W/L from 10 to 40. Samples are held in filtered clean dry air or dry nitrogen. The stress is applied as a series of gate voltage pulses between 0 and −30 or −40 V, usually with a pulse length of 300 μs, frequency of 17 Hz (60 ms repetition time), and duty cycle of 1/200. These measurement conditions are the same as used in a recent publication which gives further details of the measurement.[6] Some different frequency pulsing conditions are used for the measurements, which are described below. The V_T shift and mobility are measured from the intercept and slope of the transfer characteristic in the linear regime with a drain voltage of −5 V, and in saturation at a drain voltage of −30 V, for which the slope is measured from the square root of the current. The data are fitted over a 10 V range of gate voltage from about 10 V beyond threshold. For measurements at the shorter stress times, the voltage range over which the slope is measured is modified to account for the V_T shift. At longer times, the voltage range for the fit is kept constant even though the V_T shift appears to decrease, for reasons that are explained below.

Figure 1 shows the measurements of the apparent TFT mobility induced by gate bias stress in four PQT-12 TFT samples on the same substrate, two of which were biased at −30 V and two at −40 V. For these data and in other figures in the paper, the time refers to the total elapsed time of the measurement, rather than the time that the gate voltage is turned on which is smaller by a factor of the duty cycle. The measurements extend over 270 days with the samples held in the dark in clean dry air at room temperature. There is a steady decrease in the mobility extracted from the transfer characteristics measured in the linear regime. The solid line fit to the data is an exponential decay with the time constant indicated in Fig. 1. The time constants are of order 1–2 years and are larger at −30 V bias compared to −40 V. Hence, the rate of change of mobility increases with bias voltage. The two samples at −40 V bias show considerable difference in their time constant and there is a similar variation in measurements of other samples. Some of the mobility data in Fig. 1 show a faster initial decrease over the first few days, and previously measured samples of PQT-12 also

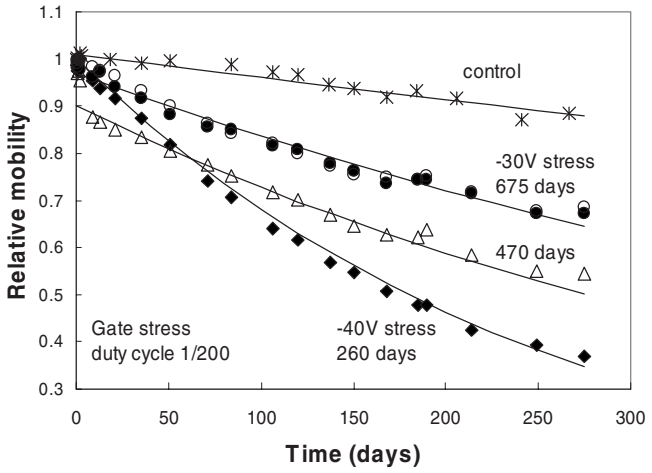

FIG. 1. Time dependence of the effective mobility (slope of linear transfer characteristics) measured in PQT TFTs at room temperature with −30 and −40 V gate biases. The solid line is a fit to an exponential decay with time constant indicated. The channel lengths of the TFTs are 15 and 20 μm for the −30 V data and 20 and 50 μm for the −40 V data.

showed an initial drop in mobility.[6] Control measurement on unstressed samples on the same substrate measured shows a mobility decrease of no more than 10% over the 270 day time period, while the stressed samples change mobility by 20%–50%.

Measurements at elevated temperature show an increased rate of the reduction in mobility and more clearly show the gate stress effect. Figure 2(a) shows the data for a PQT-12 sample at room temperature, 50 °C and 70 °C, measured over a period of 5 days under the same stressing conditions as the data in Fig. 1. The rate of decrease in mobility is more rapid as the temperature increases, and at 70 °C, the mobility has dropped by 80% in 3 days at a gate bias of −40 V. The corresponding data measured with a −30 V gate bias were qualitatively similar, but the time constants are longer by a factor of 2–3. The data in Fig. 2(a) also show that there is no measurable recovery after the stress is removed, when the sample is held at 50 °C for 2 days. Further measurements found that annealing to 100–120 °C for 10 min also does not recover the mobility.

The solid lines in Fig. 2(a) are fits to an exponential decay of mobility with time, $\exp(-t/\tau_M)$, and to a good approximation, a single time constant τ_M describes the decay, apart from the initial drop. Figure 3 shows the temperature dependence of the measured time constants and includes data at −30 and −40 V biases. The mobility decrease is consistent with a thermally activated process described by

$$\tau_M = \tau_0 \exp(E_M/kT). \quad (1)$$

The activation energy E_M is about 0.6 eV and the prefactor τ_0 is in the range of 10^{-4}–10^{-3} s. The time constant for −30 V bias is about three times that at −40 V, and E_M is the same within experimental uncertainty.

Similar measurements were made on samples of the polythiophene PBTTT. Initial unstressed measurements gave mobility of 0.06–0.15 $\mathrm{cm}^2/\mathrm{V\,s}$, which is about 50% higher than is typical for the corresponding PQT-12 samples. The data in Fig. 2(b) show a qualitatively similar bias induced decrease in mobility as in PQT-12 and a similar temperature depen-

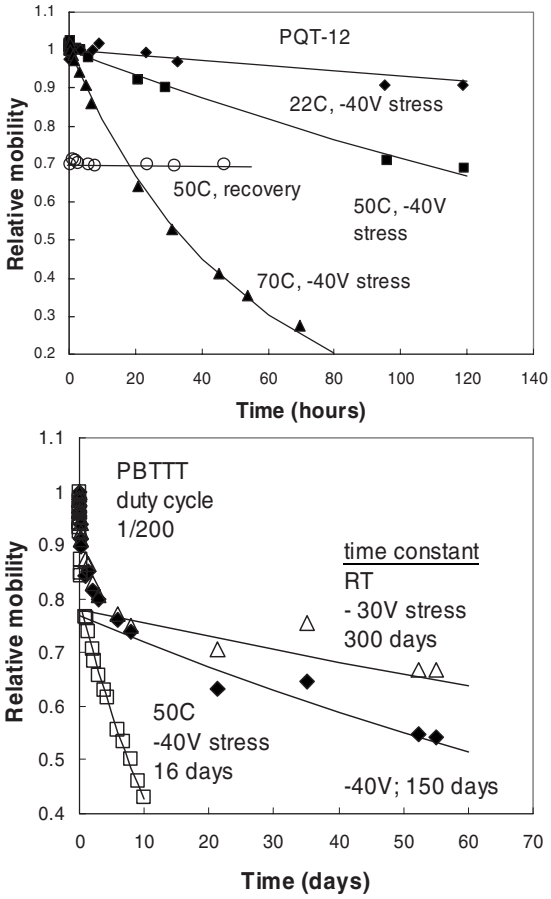

FIG. 2. Time dependence of the effective TFT mobility. (Top) PQT TFTs at −40 V gate bias measured at RT, 50 °C, and 70 °C. The lack of recovery for a sample held at 50 °C without gate bias is indicated. (Bottom) Similar data for a PBTTT TFT measured at RT and 50 °C.

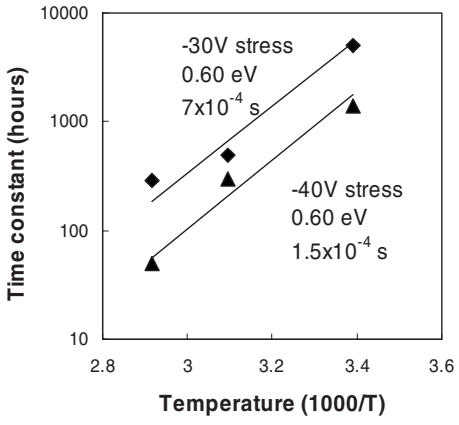

FIG. 3. Temperature dependence of the time constant for stress-induced reduction of the effective mobility, at −30 and −40 V gate bias, measured at room temperature, 50 °C, and 70 °C. The slope and intercept are indicated.

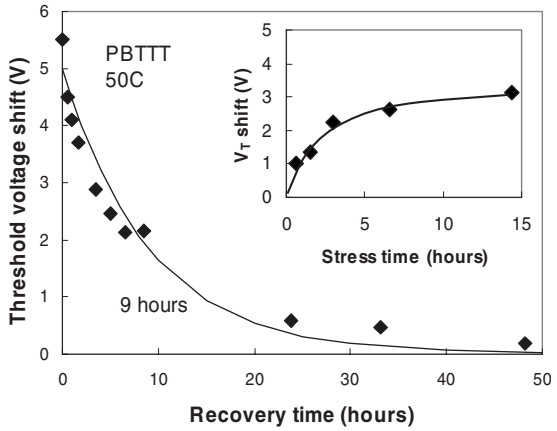

FIG. 4. Recovery of the threshold voltage shift in PBTTT at 50 °C, showing a recovery time constant of 9 h. The inset shows the increase in the V_T shift when the bias stress is applied, with saturation occurring in 10–20 h.

dence. However, in this sample, there is a larger initial fast decrease in mobility of about 20% in the first 2–3 days at room temperature, followed by a slower decline with slightly faster time constants compared to PQT-12. The PBTTT samples also exhibit a threshold voltage shift which is similar to PQT-12 in that it stabilizes after 1–2 days of stress at room temperature and recovers when the stress is removed. For the samples measured, the magnitude of the V_T shift is smaller by about a factor of 1.5–2 than is typically observed in PQT-12.

During all these stress measurements, the threshold voltage first increases and then saturates, as previously observed. For long stress times, the threshold voltage appears to decrease again, as discussed in more detail below. At elevated temperatures, the V_T shift more quickly saturates and more quickly recovers after the stress is removed. Recovery data for a PBTTT sample are shown in Fig. 4, and the V_T shift recovery time is about 9 h at 50 °C, with a similar time for stabilization of the V_T shift after the stress is applied. Similar time constants are found for PQT-12 as compared to values of about 50 h at room temperature.[6]

Current-voltage characteristics

The current-voltage characteristics were explored in more detail to gain information about the origin of the change in mobility. Examples of the linear regime transfer characteristics are shown in Fig. 5 for various stages of stress in a PBTTT TFT with 5 μm channel length and measured at 50 °C with −40 V bias. The initial data (dashed line) are measured after a short stress time when the threshold voltage shift has stabilized to a constant value, and the mobility has not changed much. The remaining data are for stress times of up to 10 days. With increasing stress time, the current in the turn-on region at low gate voltage remains unchanged, while there is a substantial decrease in current at higher gate voltage. The shape of the transfer curves also changes—the initial curvature flattens out and eventually curves in the opposite direction. When the samples are allowed to relax without

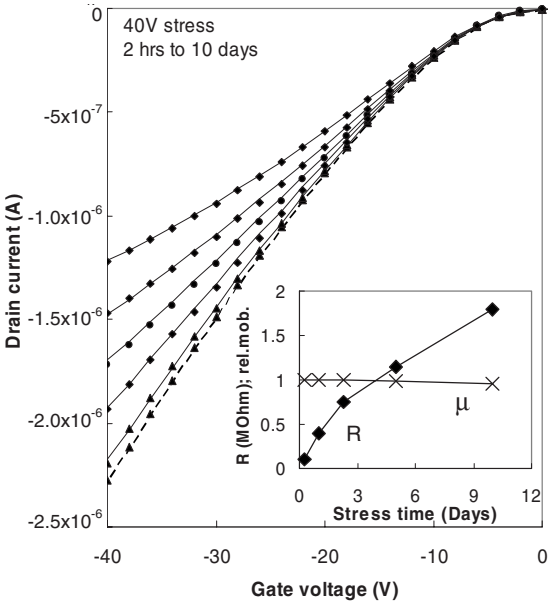

FIG. 5. Transfer characteristics for a 5 μm PBTTT TFT for different stages of stress measured at 50 °C, showing fit to a model in which the device has an increasing series resistance. The resistance and μ^* values as a function of stress time are indicated in the inset.

stress for a few hours, the turn-on region moves back to the original gate voltage of the unstressed sample, indicating that the threshold voltage has recovered, but the overall shape of the transfer characteristics is unchanged, showing that the current decrease does not recover.

The change of shape in the transfer data in Fig. 5 clearly does not represent a uniform decrease in mobility. In fact, it is a characteristic of the addition of a series resistance R_S, which can be modeled by reducing the drain voltage by the amount dropped across the series resistance. Including an additional reduction μ^* of the bulk mobility, the drain current I_D after the stress-induced changes is given by

$$I_D(V_G,\text{stress}) = \frac{\mu^* I_{D0}(V_G)}{(1+\mu^* I_{D0}(V_G) R_S/V_D)}, \tag{2}$$

where I_{D0} is the drain current of the initial state of the TFT. The solid lines in Fig. 5 show that the data fit Eq. (2) with an increasingly large series resistance with stress time and no significant change in μ^*.

Other samples show changes in both R_S and μ^*, and examples are given in Figs. 6 and 7 for measurements at 50 °C. Figure 6 shows the data from a sample from the same substrate as in Fig. 5, but with a 50 μm channel length. Again, the first data set is measured after the normal threshold voltage shift is stabilized and the data at longer stress times are fitted to Eq. (2), and the fitting values for both R_S and μ^* are shown in the inset. In this case, there is a significant decrease in μ^* and a slightly smaller increase in R_S. The data in Fig. 7 are for a PBTTT TFT also with 50 μm channel length but from a different substrate. This sample had a higher mobility and lower initial contact resistance than the samples of Figs.

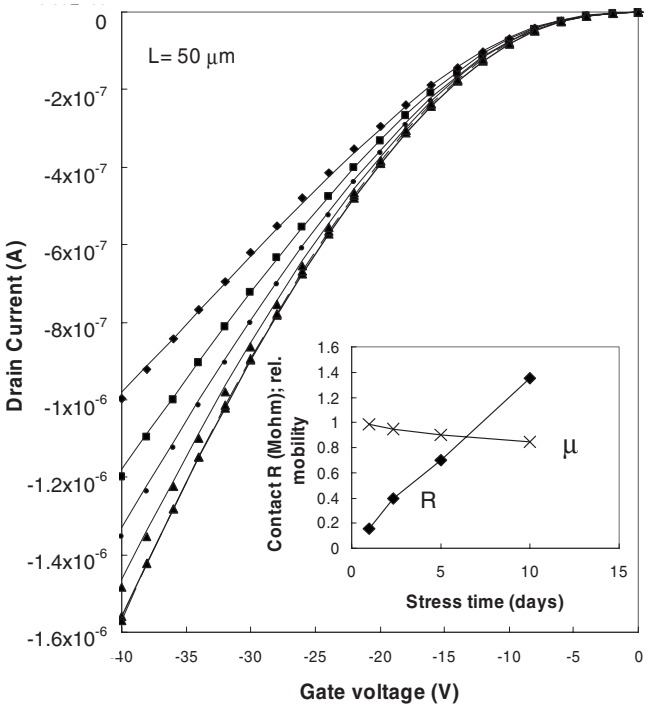

FIG. 6. Transfer characteristics for a 50 μm PBTTT TFT, on the same substrate as the sample in Fig. 4, for different stages of stress measured at 50 °C, showing fit to a model in which the device has an increasing series resistance. The resistance and μ^* values as a function of stress time are indicated in the inset.

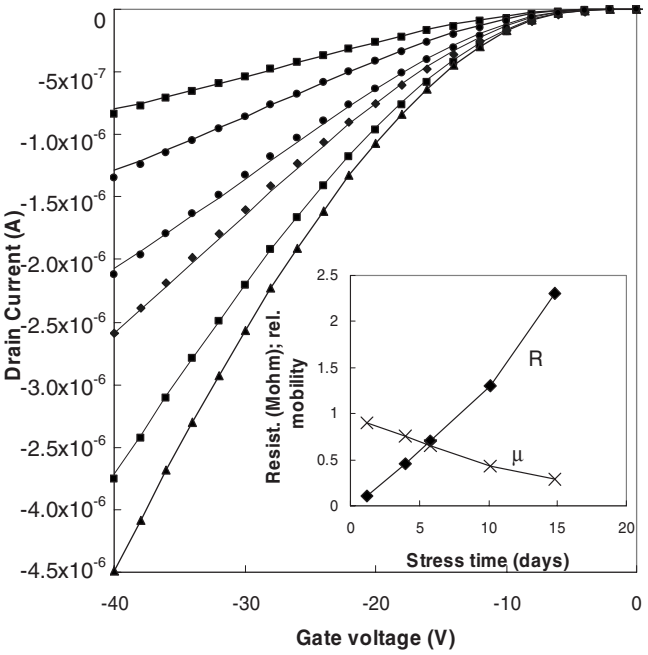

FIG. 7. Transfer characteristics for a different 50 μm PBTTT TFT for different stages of stress measured at 50 °C, showing fit to a model in which the device has an increasing series resistance. The resistance and μ^* values as a function of stress time are indicated in the inset.

5 and 6. The data are qualitatively similar, but the decrease in μ^* is larger, with $\mu^*=0.3$ at the end of the measurement, and the increase in R_S is similar to the other samples.

Contact resistance is the obvious explanation for the series resistance.[11] The data in Fig. 5 were measured on the TFT with the shortest channel length, 5 μm, and hence more affected by contact resistance than the longer channel lengths. This sample also had a significant contact resistance in the unstressed state, roughly equal to the channel resistance in the 5 μm channel length device. Hence, it is not surprising that the stress effect would predominantly affect the series resistance. The longer channel length devices show a larger change in bulk mobility as well as the change in contact resistance. Generally, we observe that for both PQT and PBTTT, the stress-induced reduction in effective mobility could be explained by a combination of increased series resistance and reduced bulk mobility.

To explore the series resistance effect further, both the linear and saturation mobilities were measured on the same sample. The saturation mobility is generally less affected by contact resistance (see Discussion), and hence the changes should be different if a contact resistance is the origin. Figure 8 compares the two measurements for a PQT-12 sample measured at 70 °C; there is a small difference in the threshold voltage extracted for the two measurements, but the mobility is derived from the same range of gate voltage for both linear and saturation data. The linear and saturation values of mobility are identical within experimental error, which suggests that in this case, the drop in mobility is primarily a bulk rather than a contact effect. However, the analysis of the stress data shows that there is both a drop in bulk mobility and an increase in series resistance, so possibly some component of the series resistance arises from the bulk of the TFT.

Figures 9 and 10 show comparable linear and saturation data for a PBTTT device measured at 50 °C. The data in Fig. 10 are the same as those in Fig. 9 but show the results over a shorter time range. The faster initial drop in linear mobility, which is also seen in Fig. 2(b), is not accompanied by a drop

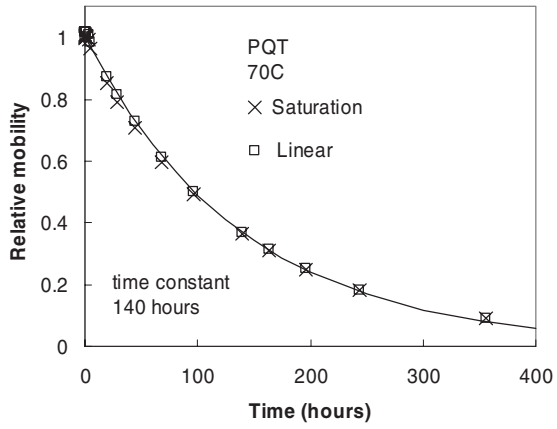

FIG. 8. Time dependence of the mobility change measured in PQT at 70 °C, comparing measurements in the linear and saturation regimes. The TFT channel length is 10 μm and the width is 200 μm. The solid line is a fit to a single exponential with time constant of 140 h.

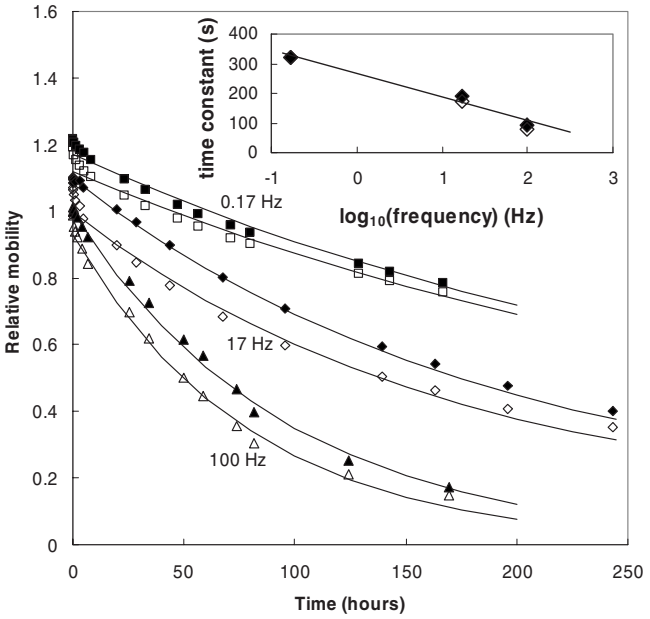

FIG. 9. Time dependence of the mobility change measured in PBTTT at 50 °C, comparing measurements in the linear regime (open symbols) and saturation (closed symbols), and for different gate pulsing frequencies as indicated. The solid lines are fits to a single exponential time constant, and the inset shows the relation between time constant and gate pulsing frequency. Each set of data is vertically offset by 0.1 units.

in the saturation mobility. However, the slower decrease at longer time has the same time constant for both linear and saturation mobilities. The data therefore indicate that there are two mechanisms present, corresponding to the bulk and contact effect, which behave differently at the beginning of the stress measurement.

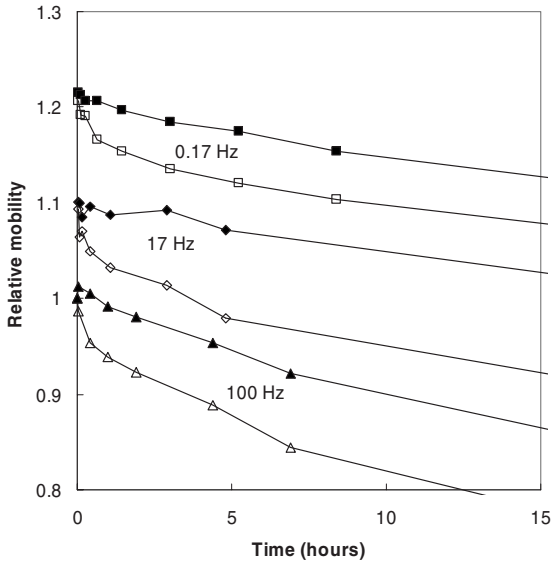

FIG. 10. Same data as Fig. 9 plotted on an expanded time scale to show the different initial response for the mobility measured in the linear and saturation regimes. Each set of data is vertically offset by 0.1 units.

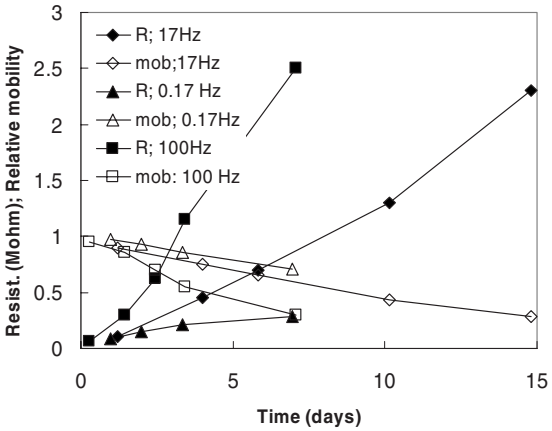

FIG. 11. Stress data for the sample use in Fig. 9, analyzed in terms of the change in series resistance R_S and relative mobility μ^*.

Figures 9 and 10 also show data for different gate stress pulsing conditions. The duty cycle of 1/200 is the same for each data set, but the frequency of the gate pulse is changed. The three data sets are from different TFTs, but they are on the same substrate. At the higher frequency, the gate-on pulse is shorter and the gate-off pulse is also correspondingly shorter, and at the lower frequency, both are longer. If the stress effect is caused by the total length of time that the gate is on, then the frequency should make no difference. As Fig. 9 shows, the bias-induced decrease in mobility is more rapid for high frequency pulsing. The difference in time constant between slow and fast pulsing rates is greater than a factor of 3. The results indicate that the number of times the gate bias is switched is an important factor in the mobility reduction.

Figure 11 shows the stress data as a function of pulsing frequency, analyzed in terms of the change in R_S and μ^*. It can be seen from the data that most of the frequency dependence arises from the change in R_S, which differs by a factor of about 5 from the highest to lowest frequency, while μ^* varies by a smaller amount. These data suggest that the frequency effect mostly relates to the contact resistance.

The change in shape of the *I-V* characteristics, which arises from the series resistance, also affects the apparent V_T shift. Figure 12 shows the V_T shift for the same measurements as in Fig. 9. At short times (<1–2 h), before there is much change in mobility, the threshold voltage similarly increases for the three gate pulse frequencies, reaching a V_T shift of about 5 V. At longer times, the V_T shift decreases again, but at a different rate for the three different frequencies. Inspection of the data in Figs. 5–7 shows that the origin of the apparent decrease in V_T shift is the change of shape of the *I-V* characteristics, and is unrelated to the usual bias-stress effect, since the onset voltage is unchanged. This is the reason that we do not correct for the V_T shift in evaluating the data after the maximum V_T shift has been reached. The fit of the data to Eq. (2) also is based on an assumption that the actual threshold voltage is unchanged.

The samples for the measurements in Figs. 9–11 were held at 50 °C for up to 1 month after the stress was removed. There was a reduction of the V_T shift by 4–5 V after a few hours, consistent with the recovery of the normal bias-

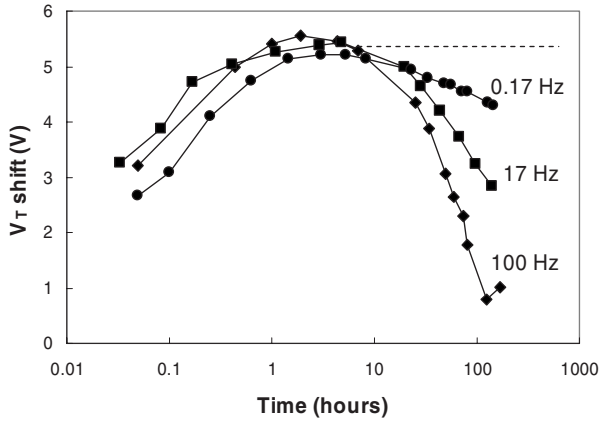

FIG. 12. Plot of the threshold voltage (V_T) shift versus time of the stress measurement, measured in the linear regime and corresponding to the data shown in Fig. 8. The decrease in V_T at long times relates to the change in shape of the transfer characteristics.

stress effect. There were no other significant changes in the *I-V* characteristics, again indicating that the stress-induced mobility change is not recovered.

III. DISCUSSION

The data show that a gate bias stress induces a decrease in TFT effective mobility which occurs with a time constant of about a year at room temperature for the biasing conditions used in the measurements and at a rapidly increasing rate at elevated temperature. The rate of change of mobility is enhanced at higher gate bias voltage and shows no recovery at least for low temperature anneals. The mechanism for the change in mobility is clearly different from that of the normal threshold voltage shift. The V_T shift stabilizes after 2–3 days at room temperature and after only a few hours at elevated temperature, whereas the mobility change continues for much longer times. The decrease in V_T shift at longer stress times is an artifact of the change of shape of the transfer characteristics due to the mobility effect. Furthermore, the decrease in mobility is not recovered by low temperature anneals, unlike the normal bias-stress effect. Hence, the decrease in mobility cannot be attributed to the trapped charge.

The evolution of the shape of the transfer characteristics in Figs. 5–7 and the V_T shift data of Fig. 12 explain some earlier results related to the threshold voltage shift. We noted in the earlier publication that there was sometimes a reversal of the V_T shift after a moderately long bias-stress measurement, which we now understand and is explained by the change in slope of the *I-V* characteristics due to the stress-induced series resistance. Our conclusion is that the normal threshold voltage shift monotonically increases and saturates to a constant value and that subsequent changes are an artifact of the change of shape due to a different mechanism.

A. Contact resistance effects

It is useful to understand the contact resistance effects in the linear and saturation regimes. Equation (2) applies to the linear regime, and the result is independent of whether the contact resistance is at the source or drain contact or a combination of both. In the saturation regime, the contact resistance effect is different for source or drain. A contact resistance at the drain increases the saturation voltage but does not change the saturation current. The reason is that in saturation, the channel potential near the drain is V_G-V_T, irrespective of whether there is drain contact resistance R_{CD}, and so the saturation current is unchanged. However, to reach saturation, the drain voltage must be at least $I_D R_{CD}$ larger than the channel potential. Hence, the saturation voltage increases.

The effect of a contact resistance R_{CS} at the source is obtained from a solution to the field-effect transistor equation allowing for a voltage drop V_X at the source,[12]

$$I_D L = C_G \mu W \int_{V_X}^{V_D} (V_{G*} - V) dV = C_G \mu W |V_{G*} V - V^2/2|_{V_X}^{V_D}, \tag{3}$$

where $V_{G*}=V_G-V_T$ and $V_X=I_D R_{CS}$. Saturation occurs when $V_D=V_{G*}$,

$$I_{DSAT} = \frac{C_G \mu W}{2L} [V_{G*} - V_x]^2. \tag{4}$$

With the approximation that $V_X \ll V_{G*}$,

$$I_{DSAT}(V_G, \text{stress}) = \frac{I_{DSAT0}(V_G)}{(1 + 2 I_{DSAT0}(V_G) R_{CS}/V_G)}. \tag{5}$$

Provided that the contact resistance is Ohmic with respect to V_D, the change is the same as that given by Eq. (2) in the linear regime. If the contact resistance is equally divided between source and drain, the current decrease in saturation should be only about half that of the linear regime because the drain contact has no effect. The contact resistance in polymer TFTs is generally not Ohmic in V_D, and instead exhibits as a curvature in the output characteristics, which is associated with a diodelike effect at the contact, in which the contact resistance decreases as the current increases.[12] Hence, the contact resistance in saturation is generally smaller that in the linear regime. This property is one reason why organic TFTs almost always exhibit a larger mobility in saturation compared to the linear regime.

The observation in Fig. 10 that the linear mobility abruptly drops at short stress times (<10 h at 50 °C), but the saturation mobility does not, is an indication of an induced contact resistance at the source and drain contacts rather than a change in bulk mobility. At longer times, the changes can be attributed to both the series resistance and the bulk mobility.

B. Mechanisms

To summarize, the gate-induced decrease in mobility is unrelated to trapped holes, is stable for low temperature annealing, occurs in both dry nitrogen and dry air, has a strongly temperature dependent rate, and depends on the number of times the gate is switched as well as the duration

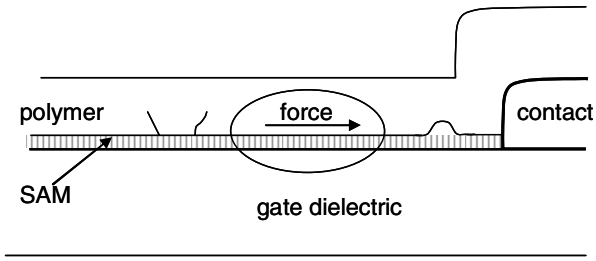

FIG. 13. Schematic figure illustrating the lateral electrostrictive effect and possible cracking or buckling effect on the polythiophene film.

of the gate bias. Part of the effect is associated with a contact resistance, and the other part is a bulk change in mobility. The insensitivity to atmosphere suggests that impurities from the ambient are not involved although we cannot exclude impurities introduced from the source material. The thermal activation of the process suggests an energy barrier to a new physical structure which is too stable to reverse.

The dependence on the gate pulse frequency suggests a possible origin for the effect. Immediately the gate voltage is applied, the capacitative coupling between the channel and the gate induces a large negative voltage in the channel. As holes flow into the channel to form the accumulation layer, the voltage rises until it is at the normal channel potential, and the gate voltage is then dropped across the dielectric. Hence, every time the gate is pulsed on and off, there is briefly a large electric field between the channel and the contacts. The time constant for the accumulation layer to form in the channel is $L^2/\mu V_{G*}$, which is of order 1 μs for these TFTs. The evidence from Fig. 9 that the pulsing frequency determines the magnitude of the effect indicates that this lateral electric field is a cause of the induced changes, rather than the gate bias across the dielectric.

A plausible physical mechanism relating the lateral field to a structural change in the polymer is the electrostrictive effect, which is a field-induced Coulomb force which tends to compress the polymer. The electrostrictive strain S_E, for a freestanding material with a voltage V across a gap d, is given by[13]

$$S_E = \varepsilon\varepsilon_o V^2/Yd^2, \tag{6}$$

where Y is the Young modulus. Polymers tend to have a high electrostrictive strain because the modulus is low.

Electrostrictive effects have been observed in polythiophene devices. Dennier *et al.* reported the measurements of the deformation of a P3HT layer in a Schottky barrier device, as the bias voltage is increased.[14,15] The field causes a measurable compression of the P3HT, although the field dependence is not exactly that given by Eq. (6). A deformation of up to 10 nm in a 1 μm film was observed.

Every time the gate is switched on or off, there is a compressive force near the source and drain contacts and a balancing tensile force in the center of the channel. It is difficult to estimate the actual force and strain in the TFT because the lateral field very rapidly changes as charge flows into the device, and the TFT is attached to the surface. If a voltage of −40 V is applied across about 1–3 μm near the contact, then the strain as calculated by Eq. (6) is of order 1% and the magnitude of the compression is ~10 nm. The calculation does not take into account that the polymer film is attached to the surface which should reduce the strain. However, there is no chemical bond to the surface and the film is actually in contact with a self-assembled monolayer which should allow some movement of the film.

We therefore propose that the change in effective mobility arises from a physical change in the structure induced by the gate bias. Aside from the lateral electrostrictive effect discussed above, two other related mechanisms can be considered. The accumulation charge in the channel provides a repulsive (tensile) Coulomb force that can also induce strain in the polymer. The third mechanism is heating by the channel current, causing thermal expansion and therefore a tensile force in the film, although we doubt that the heating is large enough given the low device current. Each of these mechanisms couples the gate field to a mechanical stress in the channel, and we cannot be sure which mechanism dominates. Figure 13 illustrates the expected effects of stress on the film, specifically for the lateral electrostrictive effect. If the stress is large enough, crack formation is expected in the region of tensile stress in the middle of the channel and buckling in the region of compressive stress.

The model is that the repetitive application of an electrostrictive force induced by gate bias switching causes a structural change in the polymer, reducing its mobility and inducing an increased contact resistance. Even though the predicted strain is small, it seems plausible that the repeated compressive stress of the long term pulsed gate (5×10^8 pulses/yr at 17 Hz) could cause a significant physical change. We speculate that the physical change (i.e., crack formation) may be most pronounced at grain boundaries in the polymer because these represent weak points in the material. We suppose that the repetitive strain causes diffusive motion of polymer chains in the region, leading to a structural change that is not removed when the gate bias is turned off. Since the electrostrictive force is between the polymer and the contacts, it is also expected that a change in contact resistance would be part of the effect. Elevated temperature is known to soften the polymer and increase chain diffusion, which could explain the strong temperature dependence of the effect.

IV. CONCLUSIONS

The data show that there is a decrease in the effective mobility induced by an extended gate bias stress in polythiophene TFTs. The mechanism is different from the bias-stress effects that induce a threshold voltage change due to hole trapping. The data suggest that the change in effective mobility is associated with a combination of a reduced bulk mobility and an increased contact resistance, which arises from a structural change in the film, perhaps caused by the electrostrictive effect.

A reduction of effective mobility obviously affects the

performance of displays or other large area electronic devices. Fortunately, the effect is relatively slow at room temperature. It would be interesting to find out if there is a similar effect in other organic semiconductors and if encapsulation or a different film thickness changes the magnitude of the effect.

ACKNOWLEDGMENTS

The author thanks M. Chabinyc for sample preparation and valuable discussions, B. Ong for providing PQT-12, and Merck for providing PBTTT. The work is performed with partial funding by the NIST Advanced Technology Program under Contract No. 70NANB3H3029.

*street@parc.com

[1] M. Matters, D. M. De Leeuw, P. T. Herwig, and A. R. Brown, Synth. Met. **102**, 998 (1999).
[2] H. L. Gomes, P. Stallinga, F. Dinelli, M. Mugia, F. Biscarini, D. M. De Leeuw, T. Muck, J. Geurts, L. W. Molenkamp, and V. Wagner, Appl. Phys. Lett. **84**, 3184 (2004).
[3] A. Salleo, F. Endicott, and R. A. Street, Appl. Phys. Lett. **86**, 263505 (2005).
[4] C. R. Kagan, A. Afzali, and T. O. Graham, Appl. Phys. Lett. **86**, 193505 (2005).
[5] S. G. J. Mathijssen, M. Colle, H. Gomes, E. C. P. Smits, B. de Boer, I. McCulloch, P. A. Bobbert, and D. M. de Leeuw, Adv. Mater. (Weinheim, Ger.) **19**, 2785 (2007).
[6] R. A. Street, M. C. Chabinyc, F. Endicott, and B. Ong, J. Appl. Phys. **100**, 114518 (2006).
[7] L. Torsi, A. Tafuri, N. Cioffi, M. C. Gallazzi, A. Sassella, L. Sabbatini, and P. G. Zambonin, Sens. Actuators B **93**, 257 (2003).
[8] R. A. Street, M. L. Chabinyc, and F. Endicott, Phys. Rev. B **76**, 045208 (2007).
[9] I. McCulloch, M. Heeney, C. Bailey, K. Genevicius, I. Macdonald, M. Shkunov, D. Sparrowe, S. Tierney, R. Wagner, W. Zhang, M. Chabinyc, R. J. Kline, M. D. McGehee, and M. Toney, Nat. Mater. **5**, 328 (2006).
[10] B. S. Ong, Y. Wu, P. Liu, and S. Gardner, Adv. Mater. (Weinheim, Ger.) **17**, 1141 (2005).
[11] C.-Y. Chen and J. Kanicki, Solid-State Electron. **42**, 705 (1998).
[12] S. M. Sze, *Physics of Semiconductor Devices* (Wiley, New York, 1969).
[13] R. E. Pelrine, R. D. Kornbluh, and J. P. Joseph, Sens. Actuators, A **64**, 77 (1998).
[14] G. Dennier, C. Lungenschmied, N. S. Sariciftci, R. Schwodiauer, S. Bauer, and H. Reiss, Appl. Phys. Lett. **87**, 163501 (2005).
[15] G. Dennier, N. S. Sariciftci, R. Schwodiauer, S. Bauer, and H. Reiss, Appl. Phys. Lett. **86**, 193507 (2005).